ORIGINAL RESEARCH ARTICLE

Population Pharmacokinetics of Abrocitinib in Healthy Individuals and Patients with Psoriasis or Atopic Dermatitis

Jessica Wojciechowski[1] · Bimal K. Malhotra[2] · Xiaoxing Wang[1] · Luke Fostvedt[3] · Hernan Valdez[2] ·
Timothy Nicholas[1]

Abstract

Background and Objective Abrocitinib is a Janus kinase 1 inhibitor in development for the treatment of atopic dermatitis (AD). This work characterized orally administered abrocitinib population pharmacokinetics in healthy individuals, patients with psoriasis, and patients with AD and the effects of covariates on abrocitinib exposure.

Methods Abrocitinib concentration measurements ($n = 6206$) from 995 individuals from 11 clinical trials (seven phase I, two phase II, and two phase III) were analyzed, and a non-linear mixed-effects model was developed. Simulations of abrocitinib dose proportionality and steady-state accumulation of maximal plasma drug concentration (C_{max}) and area under the curve (AUC) were conducted using the final model.

Results A two-compartment model with parallel zero- and first-order absorption, time-dependent bioavailability, and time- and dose-dependent clearance best described abrocitinib pharmacokinetics. Abrocitinib coadministration with rifampin resulted in lower exposure, whereas Asian/other race coadministration with fluconazole and fluvoxamine, inflammatory skin conditions (psoriasis/AD), and hepatic impairment resulted in higher exposure. After differences in body weight are accounted for, Asian participants demonstrated a 1.43- and 1.48-fold increase in C_{max} and AUC, respectively. The overall distribution of exposures (C_{max} and AUC) was similar in adolescents and adults after accounting for differences in total body weight.

Conclusions A population pharmacokinetics model was developed for abrocitinib that can be used to predict abrocitinib steady-state exposure in the presence of drug–drug interaction effects or intrinsic patient factors. Key covariates in the study population accounting for variability in abrocitinib exposures are Asian race and adolescent age, although these factors are not clinically meaningful.

Clinical Trial Numbers NCT01835197, NCT02163161, NCT02201524, NCT02780167, NCT03349060, NCT03575871, NCT03634345, NCT03637790, NCT03626415, NCT03386279, NCT03937258.

Plain Language Summary

Abrocitinib is a drug approved in the UK and Japan for the treatment of atopic dermatitis. A population pharmacokinetic model for abrocitinib was developed based on data from 11 clinical trials that included 995 healthy individuals or patients with atopic dermatitis or psoriasis. Simulations of different patient factors, such as age, race, sex, body weight, liver function, and drug–drug interactions, were tested to examine differences in abrocitinib drug levels achieved in the body. The results of these simulations indicate that although there are some differences in abrocitinib exposure, no dose adjustments of abrocitinib are necessary based on these factors.

✉ Jessica Wojciechowski
  Jessica.Wojciechowski@pfizer.com

  Bimal K. Malhotra
  Bimal.K.Malhotra@pfizer.com

  Xiaoxing Wang
  Xiaoxing.Wang@pfizer.com

  Luke Fostvedt
  Luke.Fostvedt@pfizer.com

  Hernan Valdez
  Hernan.Valdez@pfizer.com

  Timothy Nicholas
  Timothy.Nicholas@pfizer.com

[1] Department of Global Product Development, Pfizer Inc., Groton, CT, USA

[2] Department of Global Product Development, Pfizer Inc., New York, NY, USA

[3] Department of Global Product Development, Pfizer Inc., Cambridge, MA, USA

△ Adis

Key Points

Abrocitinib is a Janus kinase 1 selective inhibitor approved in the UK and Japan for the treatment of moderate-to-severe atopic dermatitis.

A two-compartment model with parallel zero- and first-order absorption, time-dependent bioavailability, and time- and dose-dependent clearance best described abrocitinib pharmacokinetics.

Differences in race and age account for variability in abrocitinib exposures but do not necessitate dose adjustment.

1 Introduction

Abrocitinib is an oral, once-daily Janus kinase (JAK)-1 selective inhibitor [1] approved in the UK and Japan for the treatment of moderate-to-severe atopic dermatitis (AD) in patients ≥ 12 years of age eligible for systemic treatment and is under consideration for approval in this patient population in the US and other regions [2–6]; it has also been evaluated in moderate-to-severe psoriasis [7]. Abrocitinib is a Biopharmaceutics Classification System (BCS) class II drug exhibiting high permeability and low solubility. A first-in-human study previously described the pharmacokinetics (PK) and pharmacodynamics of abrocitinib in healthy individuals. Abrocitinib demonstrated rapid absorption (reaching maximum levels within 1.5 h), and steady-state plasma concentrations were achieved by day 4 after once-daily dosing [8]. The primary route of elimination of abrocitinib is via cytochrome P450 (CYP) hepatic metabolism involving CYP2C19 (53%), CYP2C9 (30%), CYP3A4 (11%), and CYP2B6 (7%) [9], and 1.0–4.4% is eliminated unchanged in urine [8].

Population PK models are pivotal tools for providing quantitative descriptions of the concentration-time profile of a drug at both the population (i.e., the average or 'population-typical') and the individual levels. Population modeling methods do not necessitate dense, consistent, structured concentration sampling per participant and can be developed based on a heterogeneous data pool from multiple studies (i.e., from phase I in healthy volunteers to phase III in the target patient population) with a variety of doses, dose frequencies, and formulations [10]. By conducting population PK analyses, demographic covariates such as body weight, sex, race, and age, in addition to data and information drawn from phase I studies conducted for

evaluating the impact of formulation changes, drug–drug interactions (DDIs), and special populations (e.g., patients with hepatic/renal impairment), can be tested and identified as key factors that explain variability between individuals [11]. Furthermore, these models are the foundation for establishing exposure–response relationships of safety and efficacy endpoints to provide a rationale for dosing decisions during drug development.

There are no published reports of a population model describing the PK of abrocitinib. The objectives of this analysis were to develop a population PK model for abrocitinib among healthy individuals and patients with common inflammatory skin conditions (e.g., psoriasis and AD) and to identify covariates that account for variability in abrocitinib exposure in the study population.

2 Methods

2.1 Ethics

The study protocols were approved by the Institutional Review Boards/Ethics Committees of the study sites and all participants provided written informed consent before participation in the studies. The studies were conducted in compliance with the ethical principles originating in or derived from the Declaration of Helsinki and conducted according to the International Conference on Harmonization Guidelines for Good Clinical Practice.

2.2 Study Population, Dosing, and Sampling Schedule

Combined data from healthy volunteers and patients recruited in 11 clinical trials between May 2013 and July 2019 were included in this analysis (Online Resource 1); it includes data from seven phase I studies in healthy volunteers, one phase II study in patients with psoriasis, and one phase IIb study and two phase III studies in patients with AD. Doses of abrocitinib ranged from 3 to 800 mg/day. Full details of the dosing and plasma sampling schedule are found in Online Resource 1.

2.3 Analytical Methods

Plasma concentrations of abrocitinib were determined using validated, sensitive, and specific liquid chromatography–tandem mass spectrometric methods by WuXi AppTec (Shanghai, China). The lower limit of quantification for abrocitinib was 1.00 ng/mL. Individuals who did not receive at least one dose of abrocitinib or did not have

at least one measurable concentration of abrocitinib were excluded. No data imputations for missing or below limit of quantification (BLQ) concentrations of abrocitinib were performed. No sampled concentrations were excluded from this analysis.

2.4 Population Pharmacokinetic Analysis

2.4.1 Software

NONMEM version VII, level 4.3 (ICON Development Solutions, Ellicott City, MD, USA) was used for model development [12]. Fixed- and random-effect parameters were estimated using the Stochastic Approximation Expectation Maximization and importance sampling algorithms with Laplacian approximation, and individual values for model parameters were obtained from empirical Bayes estimates (EBE). Perl-speaks-NONMEM (version 4.8.0) was used for bootstrap procedures. Statistical and graphical outputs were generated using the R programming and statistical language (R version 3.6.1) [13].

2.4.2 Model Development

One- and two-compartment disposition models with first-order oral absorption were evaluated as candidate structural models. Time- and/or concentration-dependent changes in clearance (CL) and bioavailability (F), such as the use of exponential models as a function of time, step functions, Michaelis–Menten elimination kinetics, or indirect response models for autoinhibition, were explored for their ability to describe non-linearity in abrocitinib PK. Parallel or sequential zero- and first-order absorption processes accounting for dissolution-rate limited absorption across the range of doses were also evaluated. Structural covariates known to be highly influential a priori were built into the structural model (e.g., allometric scaling on PK parameters using body weight [exponents of 0.75 and 1 for CL and volume of the central compartment (V_c), respectively, referenced to 70 kg]; known DDI effects on CL and F; and dose, formulation, and food effects on absorption parameters). In this model, F refers to absolute F and was fixed at 0.5977. Absolute F and the fraction of abrocitinib absorbed for a 200-mg dose of oral solution was determined in a phase 1 study (NCT03250039) of healthy male participants using a ^{14}C-microtracer approach. Intravenous data from this study were not considered appropriate for population PK modeling owing to the intravenous dose (80 μg) and sample size ($n = 5$). F was logit transformed to constrain it between 0 and 1 with the addition of covariate effects, and it was assumed that the absolute F of the oral suspension was equal to that of the oral solution. With the implementation

of absolute F into the model, PK model parameters are no longer apparent but absolute (Online Resources 2 and 3).

Interindividual variability was added to structural model parameters to account for differences between individuals in the population and was assumed to be log-normally distributed (Eq. 1):

$$P_i = \theta_P \cdot e^{\eta_i}, \tag{1}$$

where P_i is the individual value for parameter (P) in the ith participant, θ_P is the population typical value for parameter P, and η is an independent random variable describing the variability in P among participants with a mean of 0 and variance ω^2. Models with and without covariance between random effects were investigated.

A residual error model with a combination of additive and proportional effects was used to describe random unexplained variability (RUV) in abrocitinib concentrations (Eqs. 2 and 3):

$$DV_{ij} = IPRED_{ij} + \sigma_{ij} * \varepsilon_{ij} \tag{2}$$

$$\sigma_{ij}^2 = IPRED^2 * \sigma_{ij,pro}^2 + \sigma_{ij,add}^2, \tag{3}$$

where DV_{ij} is the abrocitinib concentration in participant i, at observation j, $IPRED_{ij}$ is the model-predicted abrocitinib concentration, and ε_{ij} is normally distributed with a mean of 0 and variance of 1. The scale term on epsilon is σ_{ij}^2 is a combination or proportional and additive effects on the residual error.

The M3 method was used to censor BLQ observations and adjust the likelihood accordingly [14]. There was a high proportion of BLQ concentrations (> 10%) across all dose groups, including doses examined in phase III efficacy studies. Structural model selection was guided by changes in the Akaike information criterion, standard goodness-of-fit diagnostic plots, precision of parameter estimates, and eta shrinkage.

Stepwise covariate modeling approaches (forward inclusion and backward elimination) were used to identify key intrinsic and extrinsic factors that explained differences in PK between individuals. Covariates for analysis included body weight (estimation of allometric scaling exponents), sex, age (continuous or adolescent vs. adult), race, patient type (healthy volunteers, patients with AD, patients with psoriasis), hepatic impairment (normal, mild [Child–Pugh score of 5 or 6], moderate [Child–Pugh score of 7–9]), concomitant medications (fluconazole, fluvoxamine, rifampin, probenecid), food (fasted status or high-fat meal), formulation (oral suspension, tablets), and dose (on absorption characteristics). Covariates were screened for pairwise correlation. If a strong correlation existed,

the more clinically relevant covariate continued to further analyses.

2.4.3 Covariate Model Descriptions

The effect of a categorical covariate on a parameter was represented as a discrete relationship proportional to the population parameter (or additive for effects on F). For example, the effect of sex (SEX) on a parameter (P) was described as (Eq. 4):

$$\text{Proportional effect}: P = \theta_P \cdot \text{COVSEX for COVSEX}$$
$$= \begin{cases} 1 & \text{if SEX} = 1 \\ 1 + \theta_{\text{SEX}} & \text{if SEX} = 2 \end{cases}. \tag{4}$$

Additive effect (Eq. 5):

$$P = \theta_P + \text{COVSEX for COVSEX} = \begin{cases} 0 & \text{if SEX} = 1 \\ \theta_{\text{SEX}} & \text{if SEX} = 2 \end{cases}, \tag{5}$$

where SEX has a value of 1 for male participants and 2 for female participants, and θ_{SEX} is the estimable parameter for the effect of female sex on P.

The effect of a continuous covariate on a parameter was represented as a power model (or a linear model for effects on F) referenced to the median of the observed data. For example, the effect of age (AGE) on P was described as (Eq. 6)

Power model:

$$P = \theta_P \cdot \left(\frac{\text{AGE}_i}{\text{AGE}_{\text{ref}}} \right)^{\theta_{\text{AGE}}}. \tag{6}$$

Linear model (Eq. 7):

$$P = \theta_P + \theta_{\text{AGE}} \cdot \left(\text{AGE}_i - \text{AGE}_{\text{ref}} \right), \tag{7}$$

where AGE_i is the age (years) in the ith participant, AGE_{ref} is the median age in the observed population, and θ_{AGE} is the estimable parameter for the effect of age on P.

2.4.4 Covariate Selection

Initially, candidate covariates from screening procedures were independently added to the final structural model to evaluate their individual significance in improving the fit of the model to the observed data. All covariates shown to be
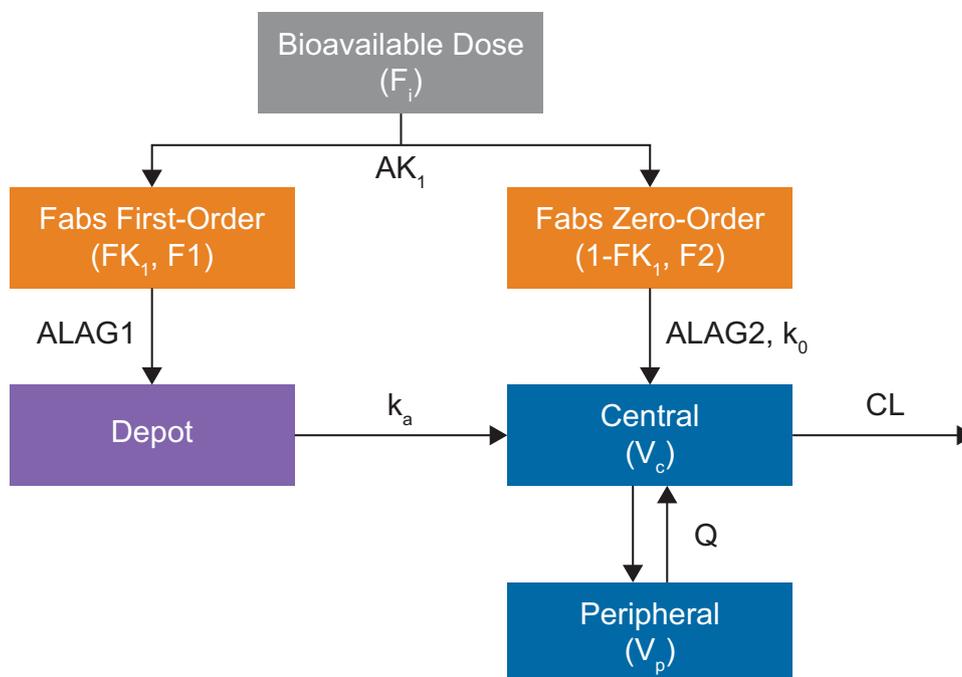
Fig. 1 Schematic representation of the final abrocitinib population pharmacokinetic model. AK_1 and FK_1 are the amount and fraction of the total dose absorbed by first-order processes, respectively. F1 and F2 are the fractions of the total bioavailable (F_i) dose that enters the depot/absorption compartment (for first-order absorption, F1) and the central compartment (for zero-order absorption, F2), respectively. The rate of absorption is dictated by the first-order rate constant (k_a) and the zero-order absorption process is dictated by the zero-order absorption rate (k_0). Absorption delays, ALAG1 for first-order absorption lag and ALAG2 for zero-order absorption lag, assume the zero-order process starts at the same time as the first-order process (i.e., where ALAG1 = ALAG2 and the processes occur in parallel) or after the first-order process has commenced (i.e., where ALAG2 = ALAG1 + ALAG2 and the processes occur sequentially). For a two-compartment model, CL is clearance from the central compartment (L/h), V_c is the volume of central compartment (L), Q is the inter-compartmental clearance (L/h), and V_p is the volume of peripheral compartment (L). *Fabs* fraction absorbed

Table 1 Pharmacokinetic analysis population characteristics by participant type

	Healthy individuals [n = 165]	Psoriasis [n = 45]	Atopic dermatitis [n = 769]	Mild hepatic impairment [n = 8]	Moderate hepatic impairment [n = 8]	Total[a,b] [n = 995]
Sex, n (%)						
Male	147 (89.1)	29 (64.4)	419 (54.5)	5 (62.5)	5 (62.5)	605 (60.8)
Female	18 (10.9)	16 (35.6)	350 (45.5)	3 (37.5)	3 (37.5)	390 (39.2)
Age group, n (%)						
Adolescent	0 (0)	0 (0)	90 (11.7)	0 (0)	0 (0)	90 (9)
Adult	165 (100)	45 (100)	679 (88.3)	8 (100)	8 (100)	905 (91)
Age, years						
Median (range)	36 (19–68)	46 (20–65)	32 (12–84)	59 (49–62)	59 (48–69)	34 (12–84)
Mean (SD)	37.6 (11)	45.7 (11.9)	35.5 (16.3)	57.9 (4.19)	58.6 (8.21)	36.7 (15.7)
Race, n (%)						
Unknown	0 (0)	0 (0)	5 (0.7)	0 (0)	0 (0)	5 (0.5)
White	99 (60)	32 (71.1)	521 (67.8)	4 (50)	7 (87.5)	663 (66.6)
Black	37 (22.4)	7 (15.6)	61 (7.9)	4 (50)	0 (0)	109 (11)
Asian	12 (7.3)	4 (8.9)	162 (21.1)	0 (0)	0 (0)	178 (17.9)
Other	17 (10.3)	2 (4.4)	20 (2.6)	0 (0)	1 (12.5)	40 (4)
Ethnicity, n (%)						
Unknown	61 (37)	0 (0)	4 (0.5)	0 (0)	0 (0)	65 (6.5)
Hispanic/Latino	15 (9.1)	3 (6.7)	28 (3.6)	0 (0)	0 (0)	46 (4.6)
Non-Hispanic/Latino	89 (53.9)	42 (93.3)	737 (95.8)	8 (100)	8 (100)	884 (88.8)
Japanese status, n (%)						
Japanese	12 (7.3)	0 (0)	32 (4.2)	0 (0)	0 (0)	44 (4.4)
Total body weight, kg						
Median (range)	80 (50.3–105)	91.2 (48.4–133)	73.9 (34.4–180)	99.2 (77.4–126)	84.2 (53.4–125)	76 (34.4–180)
Mean (SD)	79.4 (11.1)	90 (20.2)	76.9 (20.0)	96.8 (16.4)	87.5 (22.4)	78.1 (19.1)
Abrocitinib formulation, n (%)						
Suspension	109 (38.2)	0	0	0	0	109 (9.8)
Phase II tablet	24 (8.4)	45 (100.0)	0	0	0	69 (6.2)
Phase IIb tablets	0	0	192 (25.0)	0	0	192 (17.2)
Phase III tablet	152 (53.3)	0	577 (75.0)	8 (100.0)	8 (100.0)	745 (66.8)
Fed status, n (%)						
Fasted	273 (95.8)	45 (100.0)	716 (93.1)	8 (100.0)	8 (100.0)	1050 (94.2)
High-fat meal	12 (4.2)	0	0	0	0	12 (1.1)
Not controlled for food	0	0	53 (6.9)	0	0	53 (4.8)
DDI study, n (%)						
Fluvoxamine	12 (4.2)	0	0	0	0	12 (1.1)
Fluconazole	12 (4.2)	0	0	0	0	12 (1.1)
Rifampin	12 (4.2)	0	0	0	0	12 (1.1)
Probenecid	12 (4.2)	0	0	0	0	12 (1.1)
Other patient characteristics						
Creatinine CL, mL/min						
Median (range)	118 (70.5–210)	122 (68.5–260)	125 (47.1–348)	124 (80.2–190)	114 (88.4–226)	124 (47.1–348)
Mean (SD)	120 (23.1)	137 (49.4)	131 (42.9)	127 (32.4)	133 (50.7)	130 (40.7)
Albumin, g/dL						
Median (range)	4.5 (3.7–5.2)	4.4 (3.8–5.0)	4.5 (3.4–5.4)	4.35 (3.9–4.7)	3.5 (2.1–4.2)	4.5 (2.1–5.4)
Mean (SD)	4.46 (0.289)	4.42 (0.323)	4.52 (0.305)	4.31 (0.259)	3.46 (0.619)	4.5 (0.322)

Table 1 (continued)

	Healthy individuals [$n = 165$]	Psoriasis [$n = 45$]	Atopic dermatitis [$n = 769$]	Mild hepatic impairment [$n = 8$]	Moderate hepatic impairment [$n = 8$]	Total[a,b] [$n = 995$]
ALT level, U/L						
Median (range)	20 (5–58)	22 (11–55)	19 (5–92)	15 (10–42)	14 (4–39)	19 (4–92)
Mean (SD)	21.5 (9.6)	24 (10.6)	22.4 (11.8)	22.1 (13.2)	17.9 (10.7)	22.3 (11.4)
AST level, U/L						
Median (range)	21 (11–48)	21 (9–33)	22 (6–115)	20.5 (12–33)	31.5 (14–87)	22 (6–115)
Mean (SD)	22.3 (6.66)	21.1 (5.89)	23.2 (8.2)	22.2 (8.07)	38.5 (25.2)	23.1 (8.25)
Bilirubin level, mg/dL						
Median (range)	0.6 (0.1–2.0)	0.4 (0.2–1.2)	0.4 (0.2–2.0)	0.5 (0.3–1.3)	1.25 (0.4–2.6)	0.5 (0.1–2.6)
Mean (SD)	0.6 (0.249)	0.436 (0.205)	0.485 (0.254)	0.55 (0.321)	1.31 (0.702)	0.509 (0.271)

Data are expressed as n (%) unless otherwise specified

ALT alanine aminotransferase, *AST* aspartate aminotransferase, *DDI* drug–drug interaction, *SD* standard deviation

[a]The number of treatment periods exceeds the number of study individuals because some individuals were administered abrocitinib under multiple treatment conditions

[b]Summary statistics exclude missing values

important from the univariate analyses were carried forward to the multivariate analyses.

In univariate analyses, the effect of incorporating an additional covariate parameter compared with the final structural model was assessed by the likelihood ratio test. The covariate model was considered significantly better than the final structural model if $p < 0.01$. Candidate covariates also had to satisfy additional criteria: (1) 95% confidence interval (CI) of the covariate parameter estimate did not include zero; (2) addition of the covariate resulted in a reduction in interindividual variability on the target population parameter; and (3) model diagnostic plots showed improvement.

In multivariate analyses, the covariates identified in univariate analyses were added sequentially to the final structural model in order of statistical significance to form the full model. The sequential addition of a covariate to the model had to continue to fulfill the requirements described for univariate analyses. Selection of the final model was conducted by backward elimination of covariates from the full model in order of highest to lowest p values, where a covariate remained in the model if its removal resulted in a significant increase in objective function value as assessed by the likelihood ratio test ($p < 0.001$).

2.4.5 Model Evaluation

Non-parametric bootstrap analysis (stratified by study source) of the final model was performed to calculate the median and 95% prediction intervals of parameter estimates from 1000 samples. The predictive performance of the final model was evaluated by prediction-corrected visual

predictive checks based on 1000 simulations of the index data set.

2.4.6 Simulation Analyses for Evaluating the Impact of Covariates

Simulations were carried out to compare steady-state maximal plasma drug concentration (C_{max}) and 24-h area under the plasma concentration-time curve (AUC) for abrocitinib 200 mg once daily in each covariate scenario, providing geometric mean ratios compared with the reference scenario (healthy, White, adult male, 70 kg, fasted status, phase III tablet). For each covariate scenario, concentration-time profiles for 1000 trials of 30 randomly drawn individuals administered 200 mg once daily were simulated using the final model and summarized by C_{max} or 24-h AUC at steady state. The geometric mean ratios of C_{max} or 24-h AUC for each covariate compared with the reference scenario (healthy, White, adult male, 70 kg, fasted status, phase III tablet) were calculated for each trial.

The final population PK model was used to address several clinical development questions, in particular the impact of racial differences and the predicted exposures for the lower-weight adolescent population (i.e., < 40 kg) to support modification of weight-based inclusion criteria for the phase III development program. Quantitative descriptions of differences in exposure owing to (1) race (Japanese, non-Japanese Asian, other, and Western [White, Black, unknown]) and (2) weight (adolescent, adult, 25 kg, 30 kg, 35 kg, 40 kg, and 70 kg) were evaluated based on the EBE for all participants in the analysis population.

Table 2 Parameter estimates for the final population pharmacokinetic model

Parameter	Value	95% CI	Bootstrap median	Bootstrap 95% CI	Shrinkage, %
Objective function value	65,016.7	–	–	–	–
Condition number[a]	10	–	–	–	–
Population parameter					
CL, L/h	22	20.2, 23.8	21.7	17.9, 27.1	–
V_c, L	87.8	81.1, 94.5	86.3	73.7, 102	–
Q, L/h	1.16	0.994, 1.33	1.13	0.718, 1.67	–
V_p, L	8.25	7.6, 8.9	8.11	5.41, 11.5	–
k_0, mg/h	75.3	71.2, 79.4	73.1	55.1, 93.9	–
AK_1, mg	121	109, 133	122	102, 146	–
k_a, h^{-1}	4.01	3.48, 4.54	3.99	3.02, 5.41	–
RUV PRO, SD	0.437	0.429, 0.445	0.431	0.406, 0.46	–
RUV ADD, SD	0.509	0.48, 0.538	0.506	0.416, 0.599	–
Effect of moderate-variability studies on RUV PRO	0.495	0.434, 0.556	0.514	0.382, 0.636	–
Effect of high-variability studies on RUV PRO	1.16	1.05, 1.27	1.19	0.921, 1.54	–
Effect of tablet formulations on ALAG1	0.183	0.167, 0.199	0.184	0.141, 0.212	–
Effect of rifampin on CL	0.264	0.169, 0.359	0.24	− 0.0167, 1.19	–
Effect of rifampin on F	− 2.08	− 2.2, − 1.96	− 2.12	− 2.48, − 1.6	–
Effect of fluconazole on CL	− 0.541	− 0.569, − 0.513	− 0.533	− 0.61, − 0.403	–
Effect of fluvoxamine on CL	− 0.234	− 0.274, − 0.194	− 0.227	− 0.336, − 0.0594	–
Effect of fluconazole or fluvoxamine on F	1.31	1.01, 1.61	1.3	0.795, 2.13	–
Effect of high-fat meal on Ak_1	− 1	Fixed	− 1	Fixed	–
Effect of phase IIb tablets on F	− 1.02	− 1.3, − 0.744	− 1.07	− 1.49, − 0.627	–
Effect of phase III tablet on F	− 0.766	− 0.879, − 0.653	− 0.811	− 1.12, − 0.446	–
Effect of suspension on Ak_1	1.17	0.858, 1.48	1.23	0.773, 2.34	–
Effect of phase IIb tablets on Ak_1	− 0.68	− 0.776, − 0.584	− 0.685	− 0.787, − 0.233	–
Effect of multiple dosing on F	0.241	0.131, 0.351	0.253	− 0.0216, 0.698	–
Maximum change in CL with respect to time (TAFO), %	− 0.186	− 0.205, − 0.167	− 0.192	− 0.485, − 0.106	–
Rate of change in CL with respect to time (half-life), h	21.6	14.5, 28.7	23.1	8.31, 1189	–
Effect of effective daily dose on CL	− 0.169	− 0.202, − 0.136	− 0.166	− 0.227, − 0.108	–
Effect of Asian/other race on F	0.815	0.692, 0.938	0.737	0.337, 1.92	–
Combined effect of psoriasis and AD on F	0.489	0.256, 0.722	0.512	0.0678, 0.852	–
Combined effect of mild and moderate hepatic impairment on F	1.3	0.783, 1.82	1.36	0.489, 2.3	–
Effect of weight on CL and Q (referenced to 70 kg)	0.453	0.278, 0.628	0.472	0.238, 0.702	–
Effect of weight on V_c and V_p (referenced to 70 kg)	0.52	0.379, 0.661	0.524	0.341, 0.705	–
Effect of adolescent age on F	− 0.589	− 0.872, − 0.306	− 0.591	− 0.916, − 0.307	–
Effect of abrocitinib 800-mg dose on F	− 0.778	− 0.89, − 0.666	− 0.776	− 1.39, − 0.508	–
Effect of female sex on F	0.353	0.24, 0.466	0.348	0.103, 0.666	–
Interindividual variability					
ω_{CL}, % CV	57.7	51.8, 63.6	58	54, 63.2	9.71
ω_{Vc}, % CV	41.4	34.8, 48	41.5	37.4, 46.3	27.3
Correlation					
$\rho_{CL\text{-}Vc}$	0.326	0.22, 0.432	0.337	0.211, 0.454	–
Random unexplained variability					
ε_{res}	1	Fixed	1	Fixed	13.8

85.4% of bootstraps minimized successfully

AD atopic dermatitis, *AK₁* amount absorbed by first-order processes, *ALAG1* first-order absorption delay, *CI* confidence interval, *CL* clearance, *CV* coefficient of variation, *F* bioavailability, *k₀* zero-order absorption rate, *k_a* first-order absorption rate constant, *Q* intercompartmental clearance, *RUV ADD* additive residual error, *RUV PRO* proportional residual error, *TAFO* time after first dose in the occasion/treatment period, *V_c* volume of central compartment, *V_p* volume of the peripheral compartment

[a]Condition number = square root of the ratio of largest to smallest eigenvalues of correlation matrix, CV = $\sqrt{\omega^2} \times 100$, asymptotic 95% CI are presented
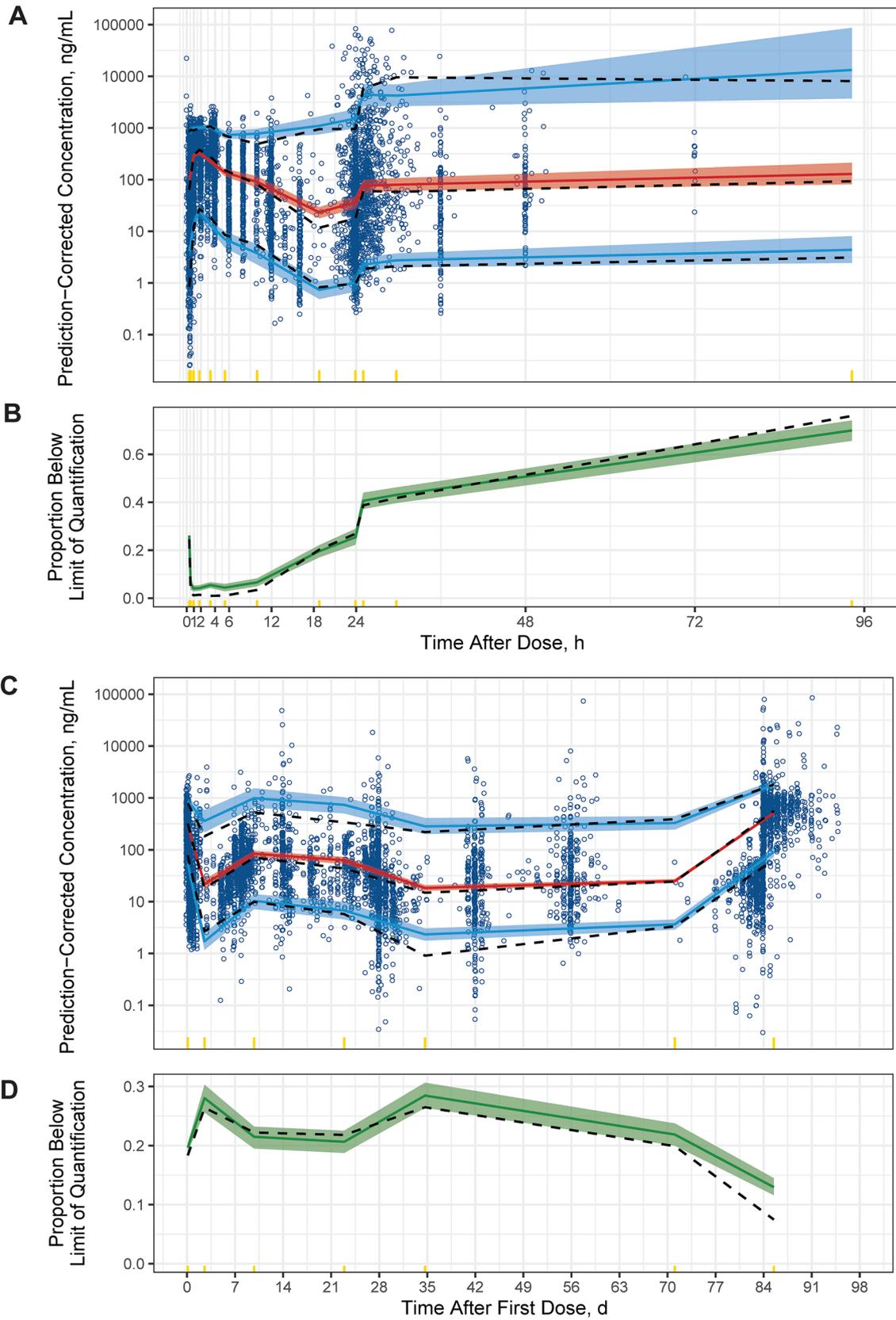
◀**Fig. 2** Prediction-corrected visual predictive check. The prediction-corrected observed data against time after dose (**a**) and time after first dose (**c**) are represented by blue circles and dashed black lines (median, 5th and 95th percentiles). The prediction-corrected simulated abrocitinib concentration (200 mg) based on the index population (*n* = 1000 simulations) are represented by the red lines and red shaded ribbons (median and 95% prediction interval of the median, respectively) and the blue lines and blue shaded ribbons (median and 95% prediction intervals of the 5th and 95th percentiles, respectively). The black dashed lines represent the proportion of observed BLQ concentrations over time after dose (**b**) and time after first dose (**d**), and the green solid line and green shaded ribbons are the median and 90% prediction intervals, respectively, of simulated BLQ concentrations (*n* = 1000) based on the index population. Yellow indicators in the *x*-axis represent the time bins for summarizing the data. *BLQ* below limit of quantification

3 Results

3.1 Sample Population Summary

The PK data set consisted of 995 individuals who contributed 6206 evaluable abrocitinib concentration measurements. Characteristics of the individuals in the abrocitinib PK analysis population are presented in Table 1. Most individuals had AD (77.3% [769/995]), were adults (91% [905/995]), and were White (66.6%). Among the total abrocitinib concentration measurements, 45.3% (2811/6206) were from individuals treated with 200 mg and 29.8% (1847/6206) were from individuals treated with 100 mg.

3.2 Structural Model Results

The final structural model was a two-compartment model with parallel zero- and first-order oral absorption with a first-order absorption lag for tablet formulations, time-dependent *F*, time- and dose-dependent CL, interindividual variability on CL and V_c with covariance between variance parameters, and a combined additive and proportional residual error model (Fig. 1). Because the overall absorption process was rapid, the ability to distinguish the sequence of zero- and first-order processes was limited. It was assumed that first-order absorption processes predominate and that zero-order processes are apparent at higher doses or with coadministration with a high-fat meal. Some formulations decreased *F* compared with oral suspension (phase IIb tablets and phase III tablet) and/or reduced the amount of a dose absorbed by first-order processes (phase IIb tablets). Rifampin, a strong inducer of CYP2C19 and CYP3A4 and moderate inducer of CYP2C9, significantly reduced *F* and increased CL. Fluvoxamine, a strong inhibitor of CYP2C19 and moderate inhibitor of CYP3A, and fluconazole, a strong inhibitor of CYP2C19 and moderate inhibitor of CYP2C9 and CYP3A, significantly increased *F* and decreased CL. Probenecid, an inhibitor of organic anion transporter 3 (OAT3), did not significantly impact abrocitinib CL. CL was shown to be time- and dose-dependent, described by an exponential model with respect to time after first dose and a power model referenced to 200 mg once daily, respectively. Michaelis–Menten elimination kinetics and autoinhibition models did not rectify bias in dose against EBE of CL. Additional increases in *F* after repeated dosing were described by a categorical variable (i.e., single or first dose vs. multiple dosing).

3.3 Covariate Analysis

Covariates that were carried forward for multivariate analyses if their inclusion improved the fit of the model at a *p* value of < 0.01 according to the likelihood ratio test reduced net variability (with the exception of the 800-mg dose on *F* but significantly improved model diagnostic plots) and were not a subset of or highly correlated with a better performing covariate, including the combined effect of Asian and other races on *F*; the effect of Japanese participants on *F* (to test whether Japanese participants were significantly different from other Asian populations); combined effect of psoriasis and AD on *F*, along with the combined effect of mild and moderate hepatic impairment on *F*; effect of estimated exponents for allometric scaling; effect of adolescent age on *F*; effect of 800-mg dose on *F*; combined effect of mild and moderate hepatic impairment on CL; and effect of female sex on *F*.

After forward inclusion and backward elimination procedures, the full model was deemed to be the final model. PK parameter estimates, bootstrap results, and asymptotic 95% CIs from the final population PK model are presented in Table 2. Final model diagnostic plots of observed vs. predicted concentrations stratified by dose are shown in Online Resource 4 and indicate that the abrocitinib PK model was consistent with observed data. The predictions of the final model overlay the observed data with good agreement and adequately reproduce the proportion of BLQ observations (Fig. 2).

3.4 Impact of Covariates on Abrocitinib Exposure

The impact of intrinsic (sex, age, race, body weight, patient status, hepatic function) and extrinsic (DDIs, fed status) factors on steady-state C_{max} and 24-h AUC based on geometric mean ratios compared with the reference scenario are shown in Fig. 3. Adolescence (with weight 70 kg), rifampin coadministration, and higher body weight resulted in lower exposure, whereas Asian/other race, coadministration with fluconazole and fluvoxamine, patient population (psoriasis/AD), hepatic impairment, and lower body weight resulted in higher exposure (Fig. 3). The effects are quantified relative to the steady-state exposure of a healthy, White, adult male weighing 70 kg who received 200 mg once daily of the phase III tablet formulation under fasted conditions. The ratios

Fig. 3 Ratios of steady-state C_{max} (**a**) and 24-h AUC (**b**) after abrocitinib 200 mg QD for given covariates. For each covariate scenario on the left *y*-axis, concentration-time profiles for 1000 trials of 30 randomly assigned participants administered 200 mg QD were simulated using the full model and summarized by C_{max} (**a**) or 24-h AUC (**b**) at steady state. The geometric mean ratio of C_{max} or 24-h AUC compared with the reference scenario (healthy, White, adult males, 70 kg, fasted status, phase III tablet) was calculated for each trial. The gray-colored density distributions represent the geometric mean ratios across all trials; red numbers are the proportion of trials with ratios of < 0.8 (left) or > 1.25 (right). Black numbers on the right *y*-axis are the median (5th and 95th percentiles) of ratios for the covariate scenario. The blue shaded region is the range of geometric mean ratios from 0.8 to 1.25, and the black vertical dashed line is a geometric mean ratio of 1. Reference low and high body weights are the 5th and 95th percentiles of the analysis population. *AUC* area under the plasma concentration-time curve, C_{max} maximal concentration, *DDI* drug–drug interaction, *QD* once daily
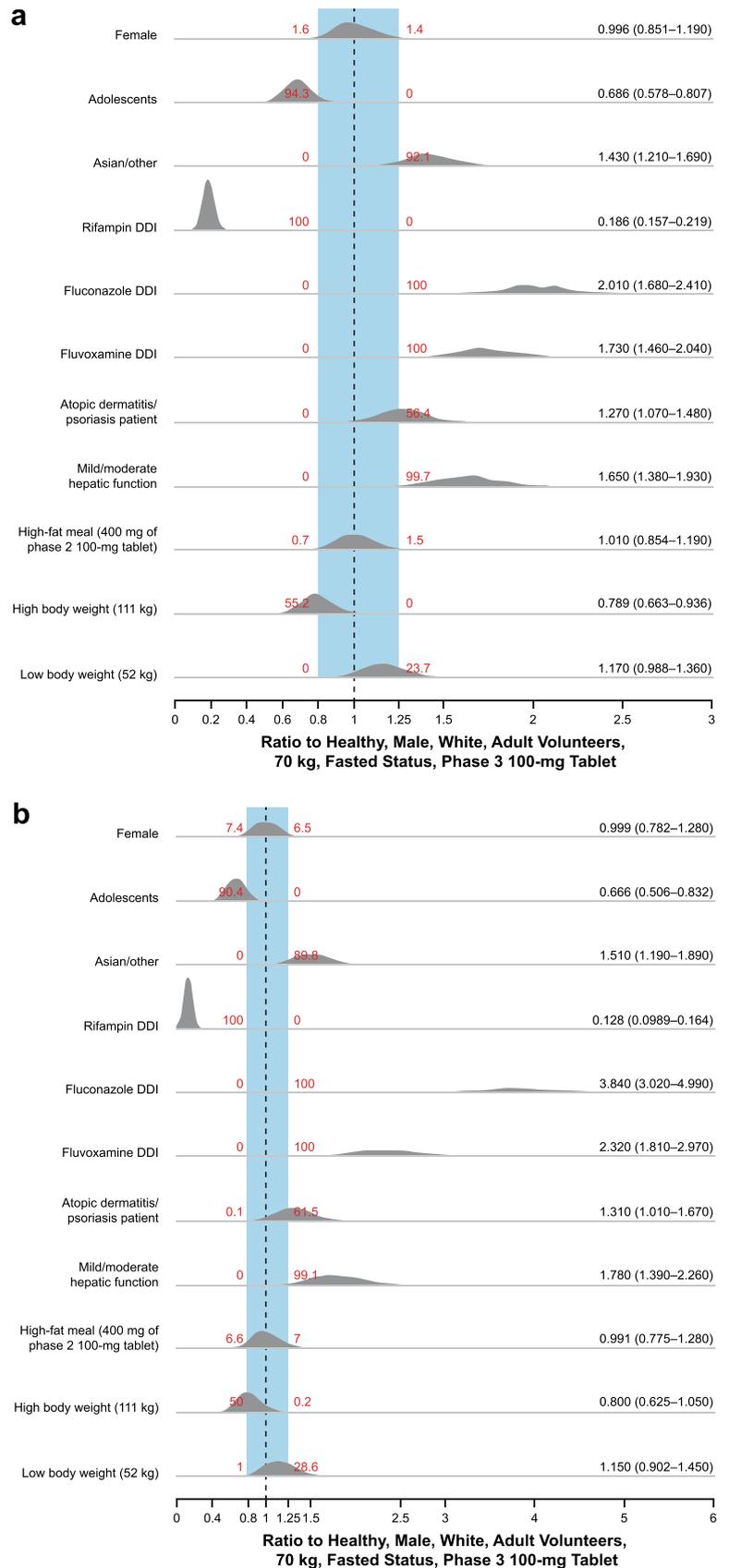
Fig. 4 Evaluation of race on abrocitinib 200 mg QD steady-state C_{max} (**a**) and 24-h AUC (**b**) for all individuals. Red circles represent the distribution of 200 mg once-daily steady-state C_{max} (**a**) and AUC (**b**) based on the EBE for all participants in the analysis population (irrespective of what dose they received), and blue box and whisker plots depict newly simulated participants ($n = 200$) based on the final population PK model. The model provides an appropriate depiction of the observed differences between the race categories. *AUC* area under the plasma concentration-time curve, C_{max} maximal concentration, *EBE* empirical Bayes estimates, *PK* pharmacokinetics, *QD* once daily
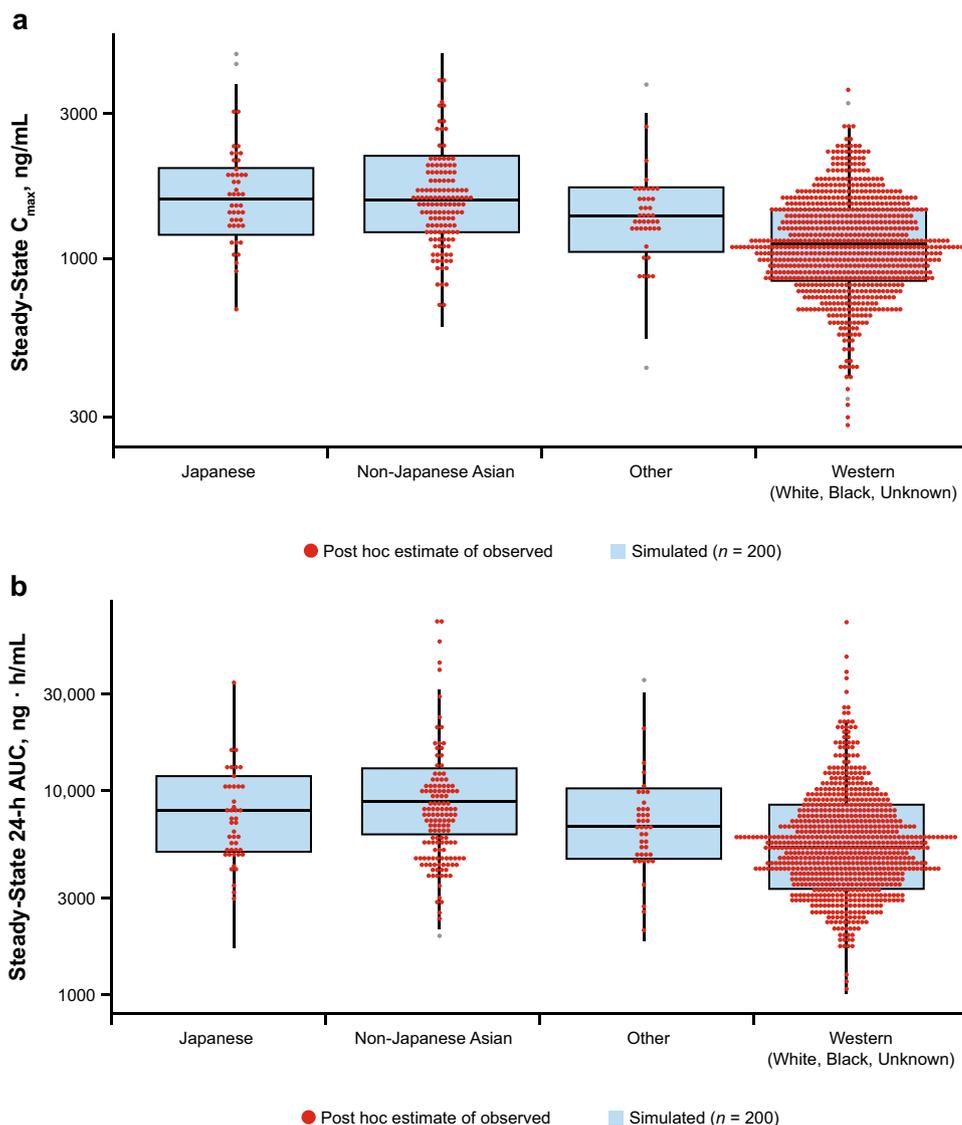
depicted in this figure are independent of other intrinsic and extrinsic factors that may also modify abrocitinib exposure. The ratios are not to be considered as additive or multiplicative to one another because combinations of covariates that are typically correlated with one another will eventually exhibit a ceiling effect because of *F* not exceeding 1.

Individuals of Asian/other race demonstrated a 1.43- and 1.51-fold increase in steady-state C_{max} and 24-h AUC, respectively, compared with the reference scenario of a White healthy volunteer weighing 70 kg (Fig. 3). After accounting for weight, race, and patient effects, the ratio of steady-state C_{max} and AUC for the typical adult Asian patient with AD who weighs 66 kg was 1.43 and 1.48, respectively, compared with a White 80 kg adult patient with AD (C_{max} of 1123 ng/mL and AUC of 5662 ng h/mL). Figure 4 shows predicted abrocitinib steady-state C_{max} and 24-h AUC for different race populations (Japanese, non-Japanese Asian, other, or Western

[White/Black/unknown]) receiving 200 mg once daily based on EBE for PK parameters. Although the central tendencies of steady-state C_{max} and AUC demonstrate that Asian populations exhibit higher exposure than Western populations, the overall distribution of the majority of Asian individuals lies within the overall distribution of their Western counterparts.

The predicted steady-state 24-h AUC and C_{max} for an adolescent patient with AD weighing 25, 30, 35, or 40 kg and for an adult weighing 70 kg after 200 mg once-daily dosing were simulated. Comparison of predicted exposures from EBE showed similarity in adolescent patients and adult patients (Fig. 5). The increases in simulated AUC and C_{max} were predicted to be approximately 27% with a decrease in body weight from 70 kg in adults to 25 kg in adolescents. This increase was considered not clinically significant.

Fig. 5 Weight-based simulations on abrocitinib 200 mg QD steady-state C_{max} (**a**) and 24-h AUC (**b**) in adolescents. Red circles represent the EBE of steady-state C_{max} (**a**) and AUC (**b**) for participants from the two phase III studies who received abrocitinib 200 mg, and blue box and whisker plots depict new simulated populations ($n = 200$) based on the final population PK model, with representative weights observed in the two phase III studies (adolescent and adult categories), test weights (25, 30, 35, or 40 kg), or reference weight (70 kg). *AUC* area under the plasma concentration-time curve, C_{max} maximal concentration, *EBE* empirical Bayes estimates, *PK* pharmacokinetics, *QD* once daily
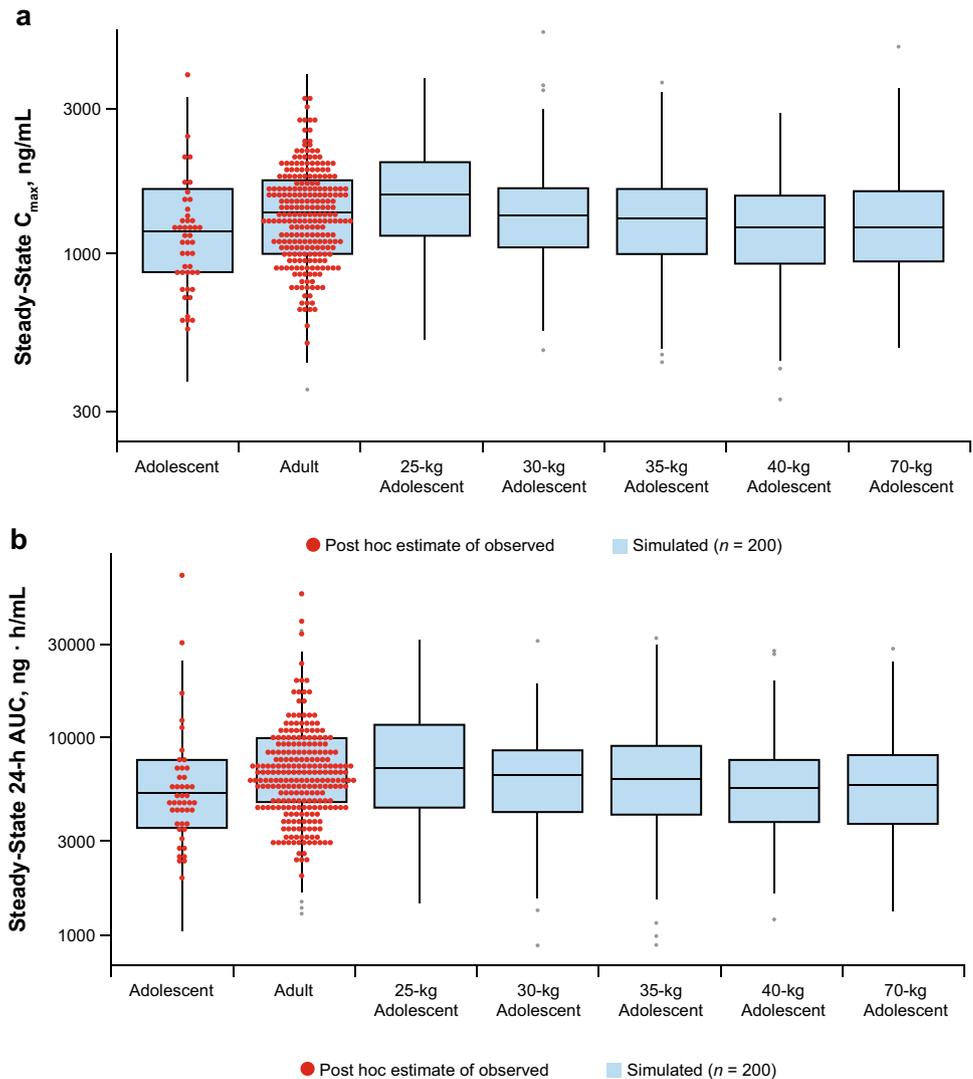
4 Discussion

This analysis characterized abrocitinib population PK based on 11 clinical trials. Abrocitinib PK were adequately described by a two-compartment model with parallel zero- and first-order absorption, time-dependent F, and time- and dose-dependent CL in the analysis population of healthy individuals, patients with moderate-to-severe psoriasis, and patients with moderate-to-severe AD. Many of the covariate effects identified in this analysis explained differences in CL and V_c by incorporation on *F*, suggesting that factors affecting the rate and extent of absorption and hepatic metabolism via the first-pass effect contribute to a significant proportion of the variability in observed concentrations. The final model provides a comprehensive evaluation of the magnitude of covariate effects (including the effects of food, DDIs, and hepatic impairment) on abrocitinib exposure in context of

the pooled analysis population. Evaluation of extrinsic and intrinsic factors using a population PK approach considers the overall variability in concentrations observed in the pooled population as opposed to the small reference cohorts or treatment arms provided by the phase 1 studies. The model serves as a platform for extrapolating the impact of covariate effects on doses or target populations, such as patients with AD, in which dedicated studies are not typically conducted.

The effect of Asian race (including Japanese) on *F* was the most significant intrinsic factor incorporated into the model to explain differences in exposure between individuals. On average, Asian participants demonstrated a 1.43- and 1.51-fold increase in C_{max} and AUC, respectively, relative to Western individuals and assuming a body weight of 70 kg. Increases in exposure via increases in *F* in Asian participants may be due to a higher frequency of CYP2C19 and CYP2C9 allele variants associated with reduced enzyme activity in this subpopulation

[15], resulting in decreased gut and first-pass metabolism of abrocitinib. In the absence of CYP2C19/2C9 genotype status for patient populations, the impact of Asian race in this analysis is possibly a surrogate for poor metabolizer phenotype. However, the presumed impact of any such polymorphism in the absence of genotypic or phenotypic information is not considered clinically significant. When accounting for differences in body weight, the ratios between a 66 kg Asian patient with AD relative to an 80 kg Western patient with AD were 1.43- and 1.48-fold for steady-state C_{max} and AUC, respectively. Although the central tendencies of C_{max} and AUC demonstrate that Asian populations exhibit higher exposure than Western individuals, the overall distribution of the majority of Asian individuals lies within the overall distribution of the Western population.

Adolescent individuals for analysis were available only from studies of patients with AD. After accounting for differences in total body weight, the exposure for a typical adolescent with AD (White, male, 61 kg) compared with a typical adult with AD (White, male, 80 kg) was 14% and 19% lower for C_{max} and AUC, respectively. In this subpopulation, it is expected that CYP metabolic capacity is mature [16, 17]. Age-related differences in gastrointestinal tract pH, volume, emptying, and transit times could possibly explain differences in oral drug absorption compared with that of adults [18]. However, the overall distribution of exposure for most adolescent individuals was similar to that of adults; therefore, adolescence is not considered a factor necessitating abrocitinib dose adjustment.

Mild and moderate hepatic impairment significantly increased steady-state C_{max} and AUC by 1.65- and 1.78-fold, respectively. The combined effect on F suggests that first-pass metabolism in these patients is impaired, resulting in more abrocitinib being available to the systemic circulation and decreasing apparent CL.

Covariate analyses indicated that patients with psoriasis and AD experienced approximately 30% higher exposure for both C_{max} and AUC at steady state compared with healthy individuals. This effect was incorporated on F in the model, suggesting increases in the fraction absorbed by or the fraction bioavailable to patients. It has been suggested that infectious and inflammatory disease states alter activities and expression of drug transporters and drug-metabolizing enzymes, such as CYP [19–23]. For a drug primarily metabolized by CYP, it is realistic to suspect that inflammation is sufficiently high in patients with psoriasis or AD to drive downregulation of intestinal/hepatic metabolism, and the first-pass effect. Covariate analyses could not distinguish between patients with psoriasis and patients with AD.

Body weight was inherently built into the structural model based on allometric scaling principles [24].

However, model diagnostics indicated an overcorrection for the impact of weight on PK parameters, and estimation of the allometric scaling exponents was tested in covariate analyses. Comparisons of steady-state ratios for different weights (70, 52, and 111 kg, population typical, 5th and 95th percentiles, respectively) demonstrated that changes in AUC were not clinically meaningful (90% prediction interval included 1) and marginally significant on C_{max}.

DDIs were well captured as part of the PK model. The modeling analysis accommodated estimation of DDI effects on CL (induction or inhibition of systemic CL) and F (changes in first-pass metabolism before entering the systemic circulation). The magnitude of changes in C_{max} and AUC for abrocitinib predicted by the final model are in agreement with the studies in which the interactions were evaluated.

The impact of renal impairment on abrocitinib PK was not evaluated because (1) 1.0–4.4% of abrocitinib is excreted unchanged in urine; (2) at the time that this population PK analysis was conducted, the concentration data from the ongoing renal impairment phase I study (NCT03660241) were not available; and (3) individuals with creatinine CL < 40 mL/min were not eligible for the phase III trials. To minimize patient burden for invasive PK sampling, obtaining blood samples in phase II/III studies was typically limited to visits associated with primary efficacy measurements after repeated dosing. Additionally, there were relatively few adolescent patients compared with adult patients, and the analysis did not assess genotype as a covariate.

5 Conclusion

A population PK model was developed for abrocitinib that can be used to predict abrocitinib steady-state exposures, dose relationships, and effects of extrinsic and intrinsic factors. Abrocitinib PK were best described by a two-compartment model with parallel zero- and first-order absorption, time-dependent F, and time- and dose-dependent CL. Covariates in the study population that account for variability in abrocitinib exposures are Asian race (increased exposure) and adolescent age (decreased exposure), although these changes were not considered clinically relevant; therefore, these patient factors do not necessitate dose adjustment.

with Good Publication Practice (GPP3) guidelines (*Ann Intern Med.* 2015;163:461-464).

Declarations

Availability of data and material Upon request, and subject to certain criteria, conditions, and exceptions (see https://www.pfizer.com/science/clinical-trials/trial-data-and-results for more information), Pfizer will provide access to individual de-identified participant data from Pfizer-sponsored global interventional clinical studies conducted for medicines, vaccines and medical devices (1) for indications that have been approved in the US and/or EU, or (2) in programs that have been terminated (i.e., development for all indications has been discontinued). Pfizer will also consider requests for the protocol, data dictionary, and statistical analysis plan. Data may be requested from Pfizer trials 24 months after study completion. The de-identified participant data will be made available to researchers whose proposals meet the research criteria and other conditions, and for which an exception does not apply, via a secure portal. To gain access, data requestors must enter into a data access agreement with Pfizer.

Code availability Not applicable.

Author contributions JW analyzed the data. All authors made substantial contributions to the interpretation of data and participated in drafting and critically revising the work. All authors approved the final version to be published and agree to be accountable for all aspects of the work.

Ethics approval The study protocols were approved by the Institutional Review Boards/Ethics Committees of the study sites, and all participants gave written informed consent before participation in the studies. The studies were conducted according to the International Conference on Harmonization Guidelines for Good Clinical Practice.

Consent to participate All participants provided written informed consent before participation in the studies.

Consent for publication Not applicable.

Trial registration These analyses included data from the following studies: NCT01835197, NCT02163161, NCT02201524, NCT02780167, NCT03349060, NCT03575871, NCT03634345, NCT03637790, NCT03626415, NCT03386279, and NCT03937258.

References

1. Vazquez ML, Kaila N, Strohbach JW, Trzupek JD, Brown MF, Flanagan ME, et al. Identification of N-{cis-3-[Methyl(7H-pyrrolo[2,3-d]pyrimidin-4-yl)amino]cyclobutyl}propane-1-sulfonamide (PF-04965842): a selective JAK1 clinical candidate for the treatment of autoimmune diseases. J Med Chem. 2018;61(3):1130–52.

2. Gooderham MJ, Forman SB, Bissonnette R, Beebe JS, Zhang W, Banfield C, et al. Efficacy and safety of oral Janus kinase 1 inhibitor abrocitinib for patients with atopic dermatitis: a phase 2 randomized clinical trial. JAMA Dermatol. 2019;155(12):1371–9.

3. Silverberg JI, Simpson EL, Thyssen JP, Gooderham M, Chan G, Feeney C, et al. Efficacy and safety of abrocitinib in patients with moderate-to-severe atopic dermatitis: a randomized clinical trial. JAMA Dermatol. 2020;156(8):863–73.

4. Simpson EL, Sinclair R, Forman S, Wollenberg A, Aschoff R, Cork M, et al. Efficacy and safety of abrocitinib in adults and adolescents with moderate-to-severe atopic dermatitis (JADE MONO-1): a multicentre, double-blind, randomised, placebo-controlled, phase 3 trial. Lancet. 2020;396(10246):255–66.

5. European Medicines Agency. SmPC for Cibinqo 2021. https://www.medicines.org.uk/emc/product/12873/smpc#AUTHDATE. Accessed 5 Nov 2021.

6. Pharmaceuticals and Medical Device Agency (PMDA) H.P. List of Approved Products in Reiwa 3rd-year October 27, 2021. https://www.pmda.go.jp/files/000240478.pdf. Accessed 5 Nov 2021.

7. Schmieder GJ, Draelos ZD, Pariser DM, Banfield C, Cox L, Hodge M, et al. Efficacy and safety of the Janus kinase 1 inhibitor PF-04965842 in patients with moderate-to-severe psoriasis: phase II, randomized, double-blind, placebo-controlled study. Br J Dermatol. 2018;179(1):54–62.

8. Peeva E, Hodge MR, Kieras E, Vazquez ML, Goteti K, Tarabar SG, et al. Evaluation of a Janus kinase 1 inhibitor, PF-04965842, in healthy subjects: a phase 1, randomized, placebo-controlled, dose-escalation study. Br J Clin Pharmacol. 2018;84(8):1776–88.

9. Dowty M, Yang X, Lin J, Bauman J, Doran A, Goosen T, et al. P190—the effect of CYP2C9 and CYP2C19 genotype on the pharmacokinetics of PF 04965842, a JAK1 inhibitor in clinical development. Drug Metab Pharmacokinet. 2020;35(1 Suppl):S80.

10. Mould DR, Upton RN. Basic concepts in population modeling, simulation, and model-based drug development-part 2: introduction to pharmacokinetic modeling methods. CPT Pharmacomet Syst Pharmacol. 2013;2:e38.

11. Mould DR, Upton RN. Basic concepts in population modeling, simulation, and model-based drug development. CPT Pharmacomet Syst Pharmacol. 2012;1(9):e6.

12. Beal SS, Boeckmann L, Sheiner LB. NONMEM User's Guides. (1989–2009). Gaithersburg, MD: ICON Development Solutions; 2009. Corpus ID: 65385267. https://www.semanticscholar.org/paper/NONMEM-User's-Guides.-(1989-2009)-Beal-Boeckmann/1964357daa9975ac959840262a810b2e0b39c8f4. Accessed 20 Jan 2021.

13. R Core Team. R: A Language and Environment for Statistical Computing. Vienna: R Foundation for Statistical Computing; 2019. Available at: https://www.R-project.org/. Accessed 20 Jan 2021.

14. Beal SL. Ways to fit a PK model with some data below the quantification limit. J Pharmacokinet Pharmacodyn. 2001;28(5):481–504.

15. Kim K, Johnson JA, Derendorf H. Differences in drug pharmacokinetics between East Asians and Caucasians and the role of genetic polymorphisms. J Clin Pharmacol. 2004;44(10):1083–105.

16. Krekels EHJ, Rower JE, Constance JE, Knibbe CAJ, Sherwin CMT. Hepatic drug metabolism in pediatric patients. In: Xie W,

editor. Drug metabolism in diseases. Boston: Academic Press; 2017. p. 181–206.

17. de Wildt SN, Tibboel D, Leeder JS. Drug metabolism for the paediatrician. Arch Dis Child. 2014;99(12):1137–42.

18. Kaye JL. Review of paediatric gastrointestinal physiology data relevant to oral drug delivery. Int J Clin Pharm. 2011;33(1):20–4.

19. Morgan ET. Impact of infectious and inflammatory disease on cytochrome P450-mediated drug metabolism and pharmacokinetics. Clin Pharmacol Ther. 2009;85(4):434–8.

20. Tanino T, Komada A, Ueda K, Bando T, Nojiri Y, Ueda Y, et al. Pharmacokinetics and differential regulation of cytochrome P450 enzymes in type 1 allergic mice. Drug Metab Dispos. 2016;44(12):1950–7.

21. Ma G, Xie R, Strober B, Langley R, Ito K, Krishnaswami S, et al. Pharmacokinetic characteristics of tofacitinib in adult patients with moderate to severe chronic plaque psoriasis. Clin Pharmacol Drug Dev. 2018;7(6):587–96.

22. Nader A, Stodtmann S, Friedel A, Mohamed MF, Othman AA. Pharmacokinetics of upadacitinib in healthy subjects and subjects with rheumatoid arthritis, Crohn's disease, ulcerative colitis, or atopic dermatitis: population analyses of phase 1 and 2 clinical trials. J Clin Pharmacol. 2020;60(4):528–39.

23. Klunder B, Mohamed MF, Othman AA. Population pharmacokinetics of upadacitinib in healthy subjects and subjects with rheumatoid arthritis: analyses of phase I and II clinical trials. Clin Pharmacokinet. 2018;57(8):977–88.